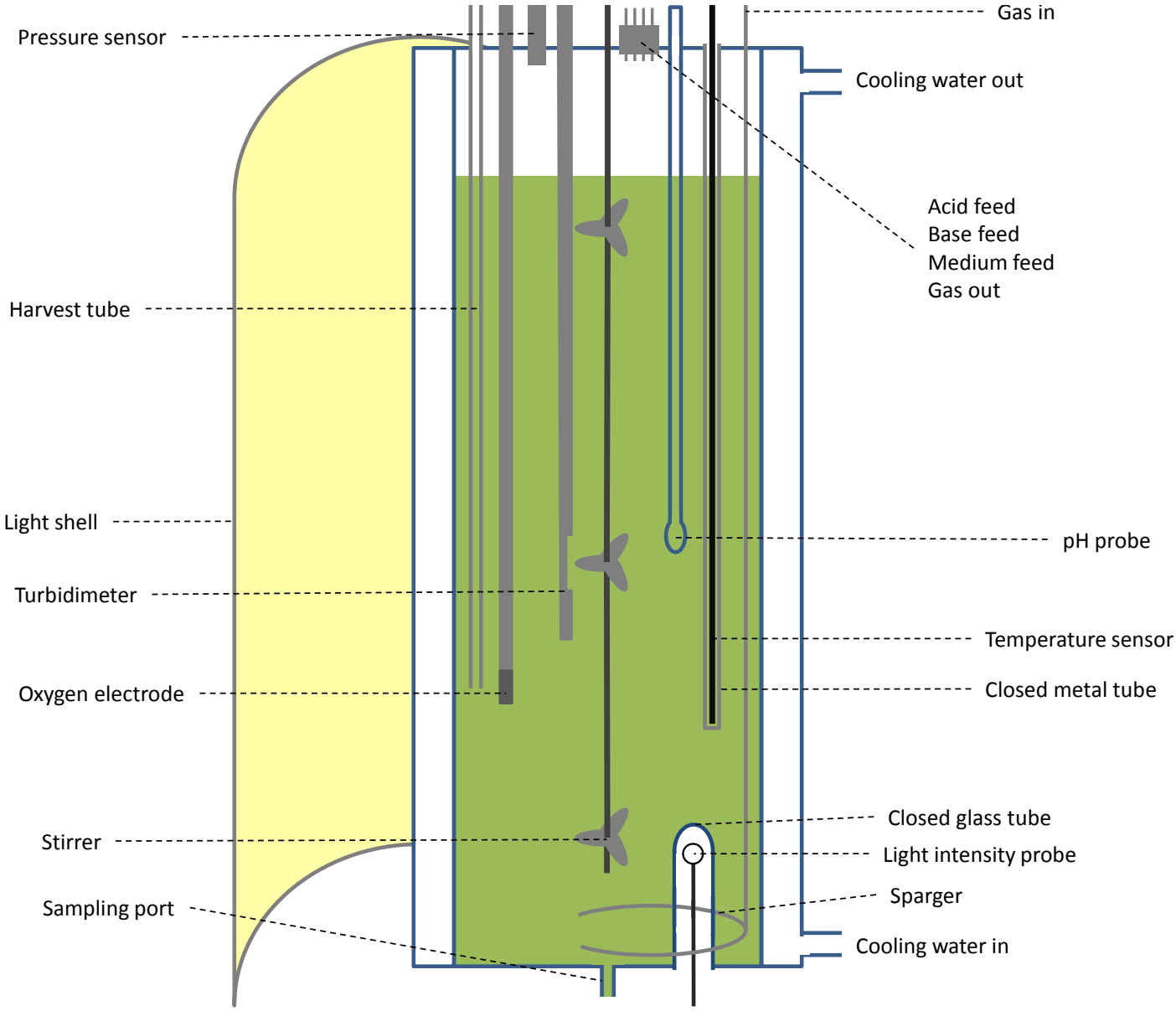

Supplemental Figure 1. Schematic Showing the Components of the Bioreactors.

5-litre bioreactors BIOSTAT®B-DCU (Sartorius Stedim, Germany) were used to grow continuous cultures. The reactors were bubbled with 200 cm^3*min^{-1} of altered 5% CO_2 in air and are stirred at 50 rpm with three impellers. Cell density was monitored by a turbidimeter, and when set threshold was exceeded (equivalent to 3-4*10^6 cells*ml^{-1}), autoclave-sterilised medium was pumped automatically into the bioreactor to dilute the culture. The entire bioreactor was set on scales, and when an increase in weight was detected from the addition of fresh medium, culture was pumped out via the harvest tube to a sterile 20 L carboy. The pH of the culture was constantly monitored, and if the pH dropped below 6.95, sterile 1 M KOH was slowly pumped into the bioreactor until the pH was within 0.05 units of 7.00. If the pH increases above 7.05, sterile 1 M HCl was pumped into the bioreactor. Temperature was also controlled, and regulated by water circulating within an outer mantle, in addition to water used to cool the light system. If the pressure within the headspace exceeds a set value, an alarm was triggered. All of these parameters, and others, like the dissolved oxygen concentration, are logged in the MFCS/win software, which also controls all parameters of the bioreactor, including light in conjunction with a second software program, Quattro Color Light is supplied from two LED half-shells and is focused with individual lenses to the centre of the bioreactor, to minimise light gradients within the bioreactor.

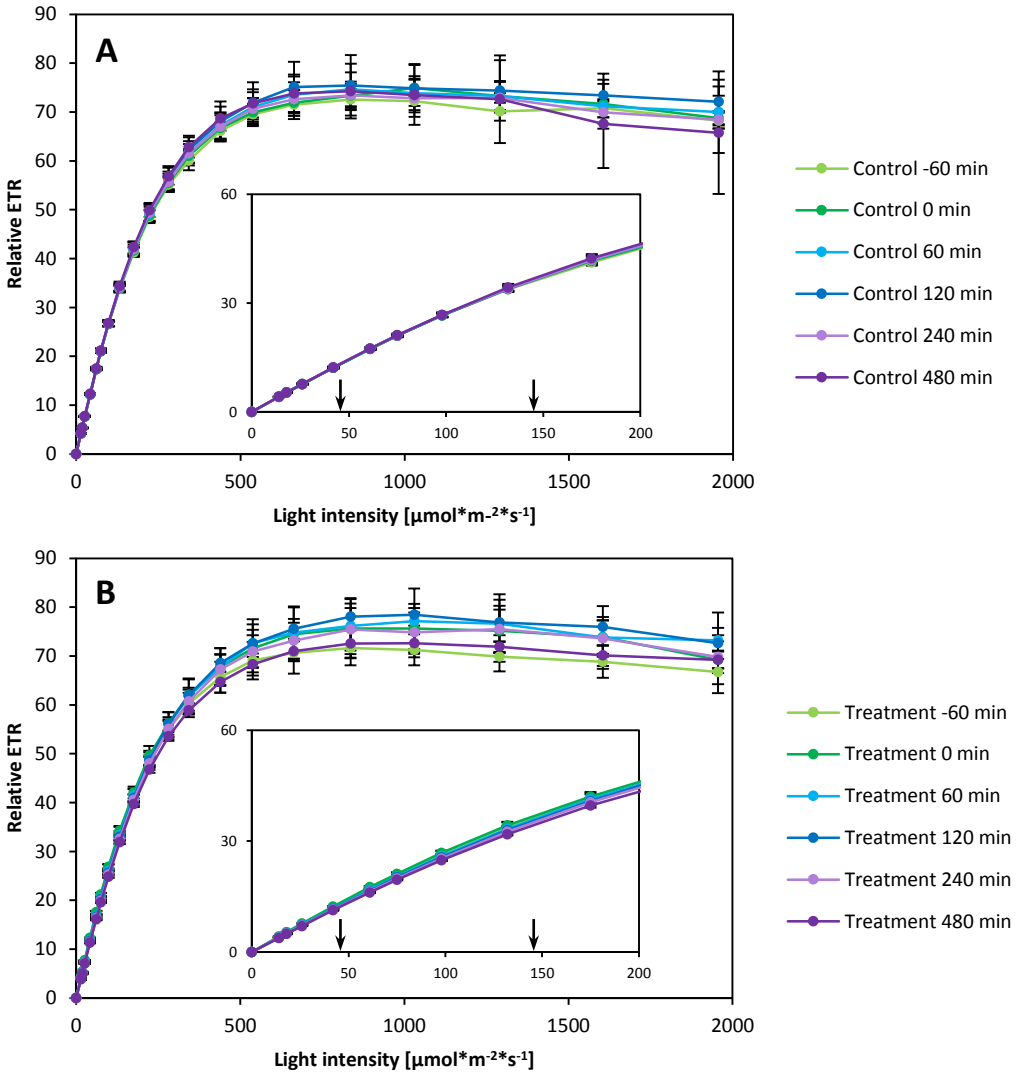

Supplemental Figure 2. Light Saturation Curves of *C. reinhardtii* CC-1690 Cells Under Low Light (A) and during the Light Shift Experiment (B).

(A) In the control conditions, light was kept at a light intensity of 41 µmol photons*m^{-2}*s^{-1} for the course of the experiment. Relative ETR was measured at -60 min, 0 min, 60 min, 120 min, 240 min and 480 min during the time course (n = 3 ± SD).
(B) In the treatment conditions, light intensity was shifted from 41 to 145 µmol photons*m^{-2}*s^{-1} at time point zero. Relative ETR was measured one hour before the light shift (-60min), just before the light shift (0 min) and 60 min, 120 min, 240 min and 480 min after the light shift (n = 3 ± SD).
Arrows in the inserts indicate growth light intensities.

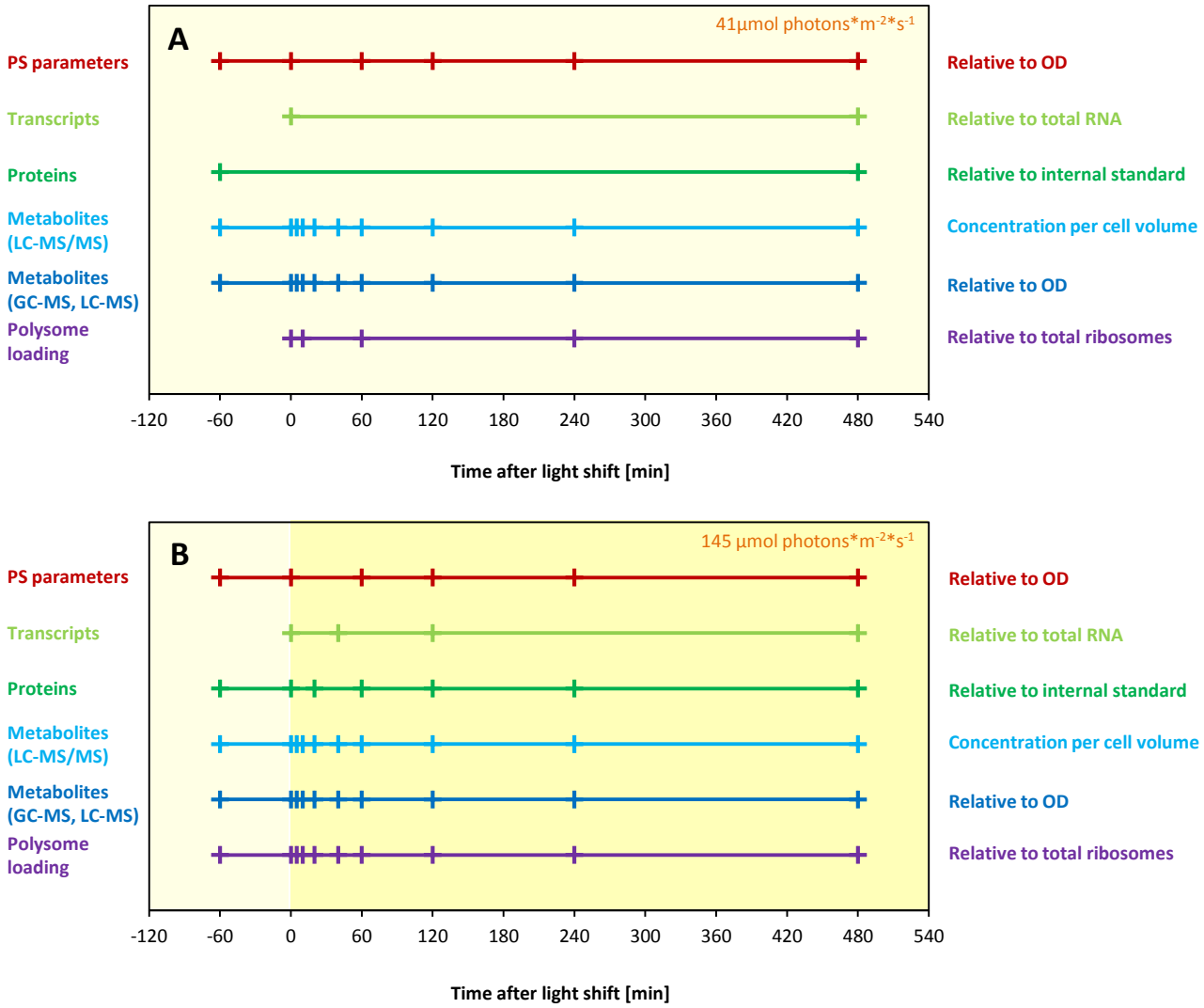

Supplemental Figure 3. Experimental Setup.

C. reinhardtii CC-1690 cells were grown continuously at 24°C, 5% CO_2 and 41 µmol photons*m^{-2}*s^{-1} for three days before the start of the experiment to assure steady-state conditions. The functional levels analysed are given on the left and the units of each level on the right side of the graph (PS, photosynthesis; OD, optical density). The time points the samples were taken for the different functional levels are indicated by vertical lines. Two (proteins and metabolites, additionally three and two technical replicates were analysed, respectively) or three (other functional levels) bioreactor runs were performed. Metabolites of the central metabolism were measured absolutely and relatively, respectively, with LC-MS/MS and GC-MS and lipids were measured relatively with LC-MS (for details, see Methods).
(A) In the control conditions, light was kept at the initial light intensity for the course of the experiment.
(B) In the treatment conditions, light intensity was shifted from 41 (light yellow) to 145 µmol photons*m^{-2}*s^{-1} (dark yellow) at time point zero.

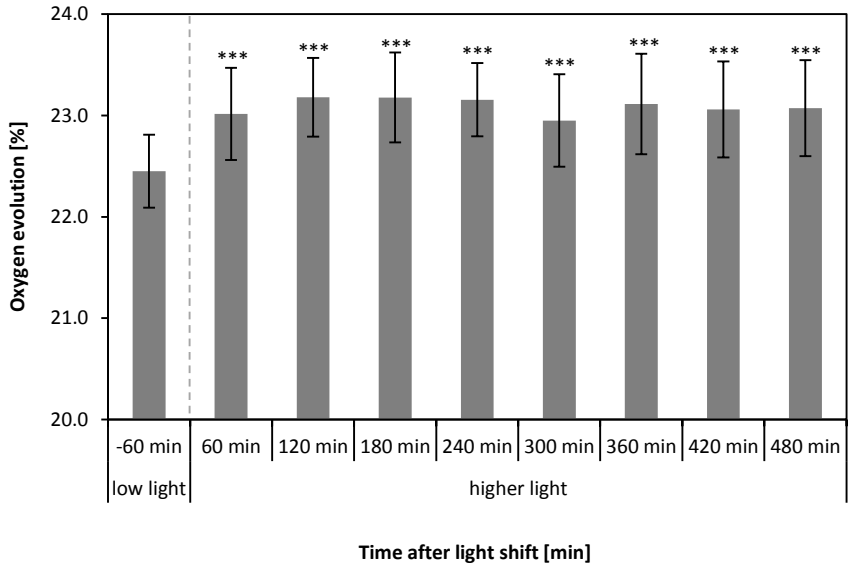

Supplemental Figure 4. Oxygen Concentration in the Outlet Air of the Bioreactor.

Oxygen concentration in the outlet air of the open-system bioreactor after the increase in light intensity at time point zero (dashed line). Additionally, the medium was pumped 2.4 times faster at the higher light intensity (n = 24 ± SD, Student´s *t*-test: three asterisks, $p<0.001$).

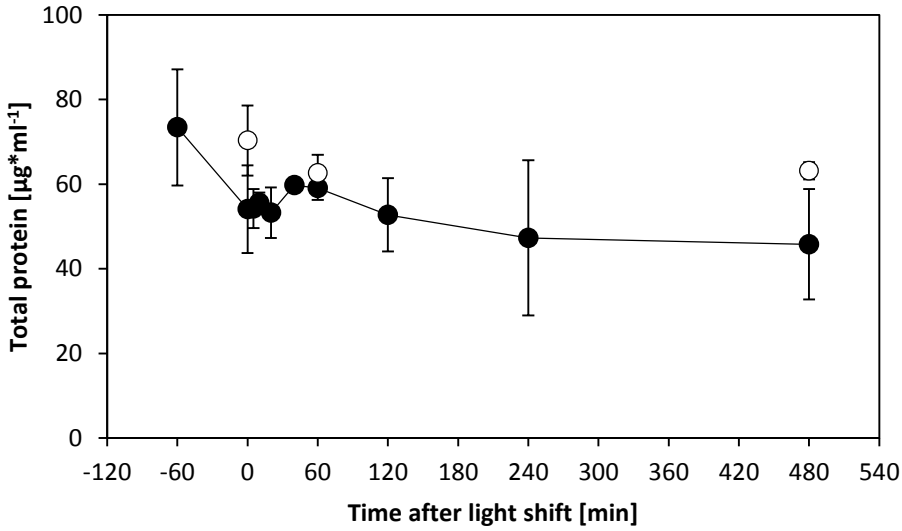

Supplemental Figure 5. Total Protein Content.

C. reinhardtii CC1690 cells were grown in a bioreactor at 24°C, 5% CO_2 and 41 µmol photons*m^{-2}*s^{-1}. At time point zero the light was either kept at the initial light intensity (open cycles, n = 2 ± SD) or shifted to 145 µmol photons*m^{-2}*s^{-1} (filled cycles, n = 2 ± SD) at time point zero. Total protein content was measured by Bradford assay as described in Methods.

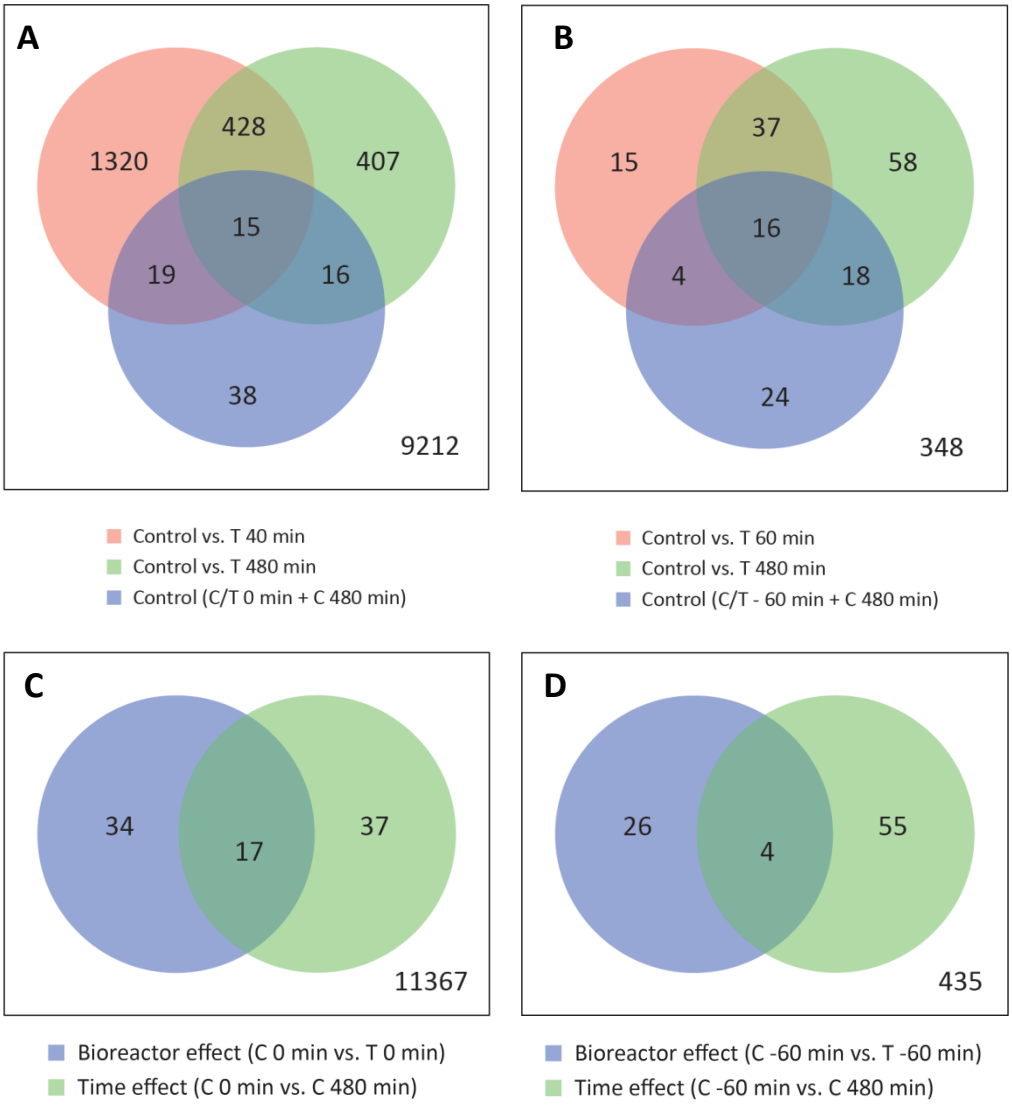

Supplemental Figure 6. Venn Diagrams Showing Numbers of Significantly Changed Transcripts (A, C) and Proteins (B, D).

Numbers in the Venn diagrams indicate significantly changed transcripts and proteins determined by using an ANOVA refined by a contrast analysis with p-value < 0.05. Additionally, a relevance threshold ($-1 \geq \log_2$ (fold change) ≥ 1) was applied to the transcript data set. C, control; T, treatment.

(A and B) Venn diagrams showing the numbers of transcripts **(A)** and proteins **(B)** significantly changed after the light shift at early (red) and late time points (green) compared to the control (blue). The control is the combination of the time points before the light shift and the 480 min time point of the untreated control bioreactor. Transcripts and proteins that differ within the control are used to check for changes over time not related to the light shift (blue, for more details, see C and D).

(C and D) Venn diagrams showing the numbers of transcripts **(C)** and proteins **(D)** significantly changing due to an effect using separate bioreactors (blue) and a time effect (green), respectively. Transcripts and proteins that significantly differ between the control and treatment bioreactors in time points before the light shift can be explained by the bioreactor effect. Changes over time in the untreated control bioreactor can be explained by the time effect. Both, the time and bioreactor effect are independent of the effect by the shift in light.

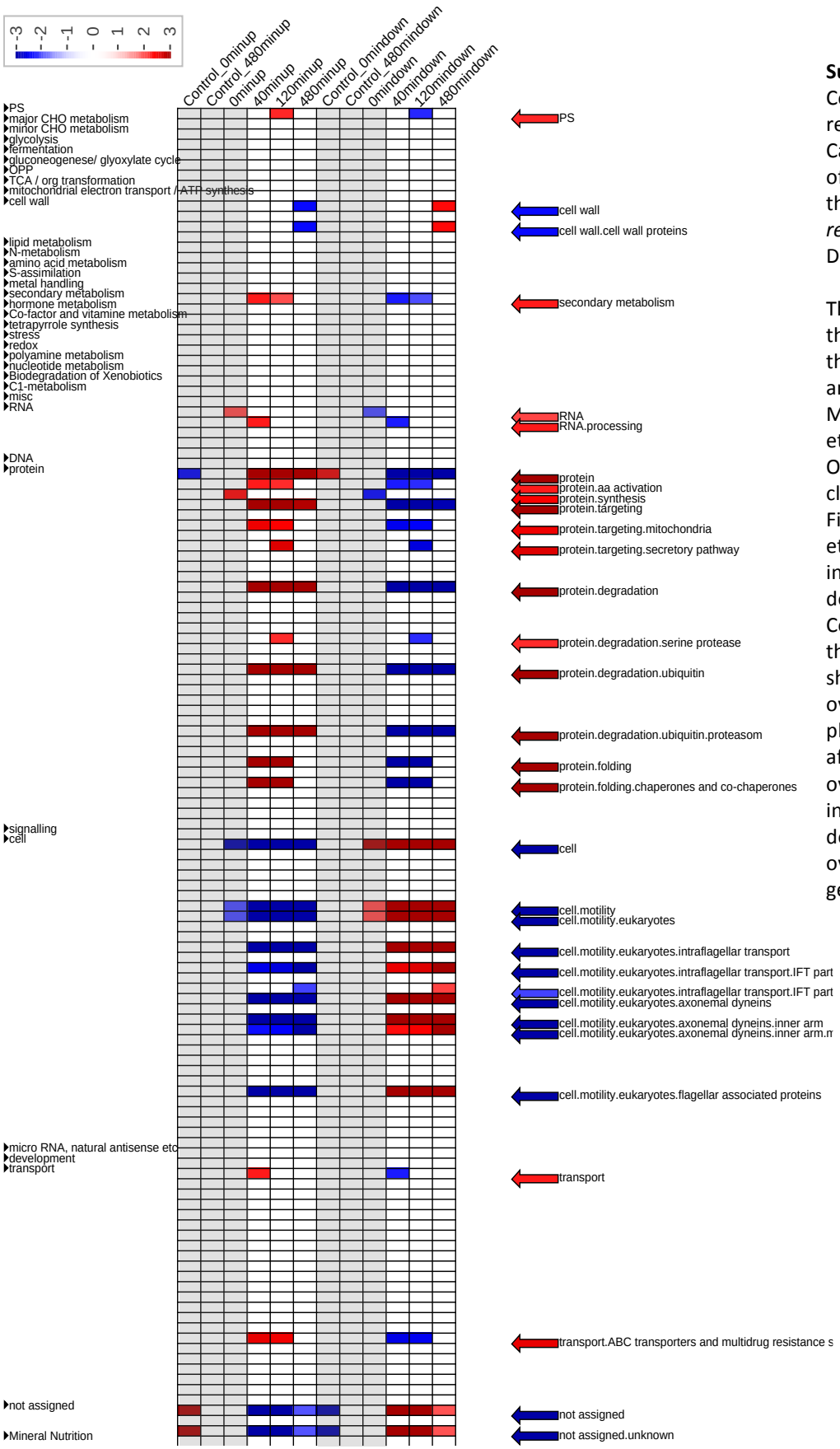

Supplemental Figure 7. Comparison of Significant Over-represented Functional Gene Categories (and Sub-Categories) of Different Time Points during the Light Shift Applied to *C. reinhardtii* CC-1690 Cells Determined by PageMan.

The values are representative of the $\log_2$ transformed values of three individual hybridizations and classed according to the MapMan classifications (Thimm et al., 2004; Usadel et al., 2005). Over-representation of classifications was assessed via Fisher test (p-value < 0.05; Usadel et al., 2006). Red indicates an increase whereas blue indicates a decrease (see color scale). Controls where light was kept at the initial light intensities are shaded in grey. Note, first, the overrepresentation for photosynthesis genes at 120 min after the light shift, second, the overrepresentation of genes involved in protein targeting and degradation and third, the overrepresentation of decreased genes involved in cell mobility.

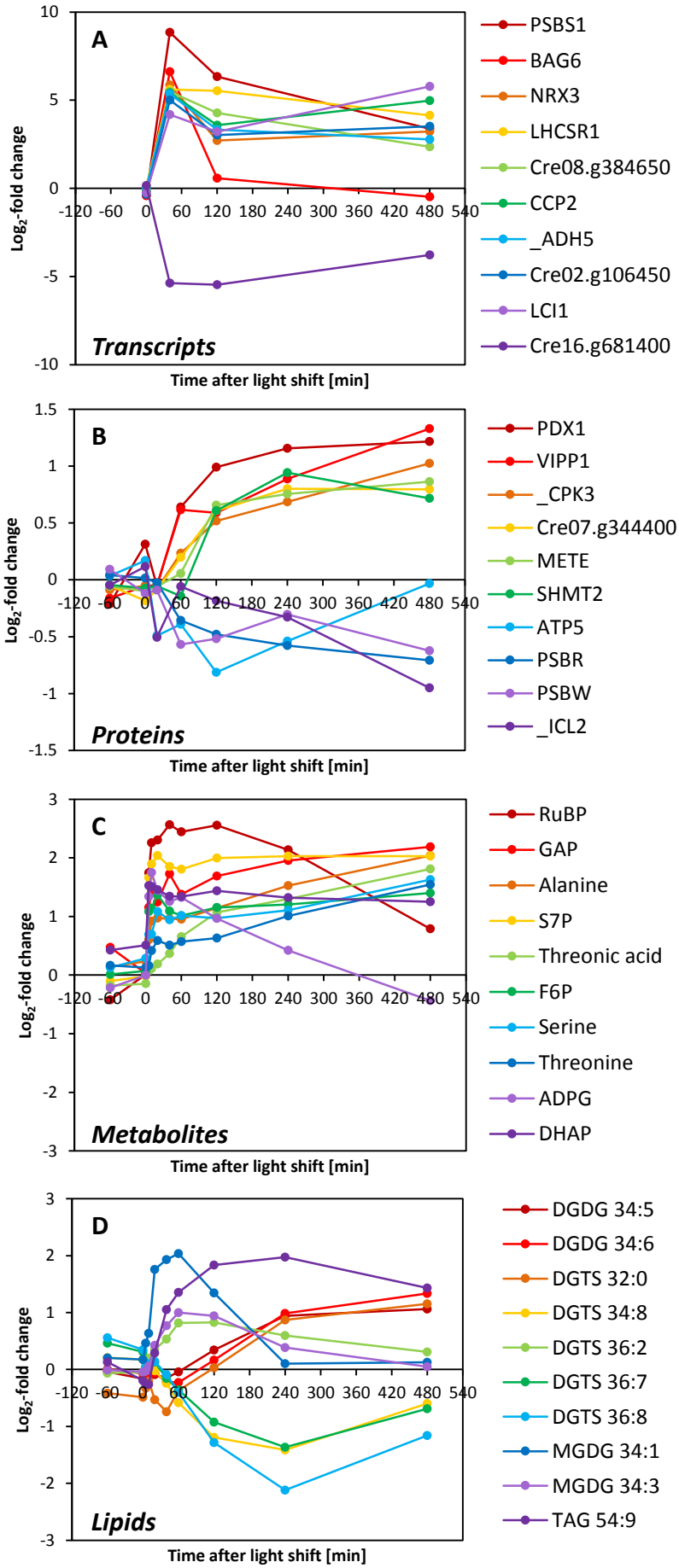

Supplemental Figure 8. Top-10 Log_2-fold Changes of Transcripts (A), Proteins (B) Metabolites (C) and Lipids (D) during the Light Shift Applied to *C. reinhardtii* CC-1690 Cells.

Log_2-fold changes were calculates for each measured time point after the light was increased from 41 to 145 µmol photons*m^{-2}*s^{-1} relative to the average of the -60 min and 0 min time points before the light was increased. For further details of analyses see Methods.

(A, C and D) The transcripts (A), metabolites (C) and lipids (D) with the ten most extreme log_2-fold changes at any time point at the higher light intensity are shown.

(B) Proteins with the ten most extreme average log_2-fold changes at the higher light intensity are shown.

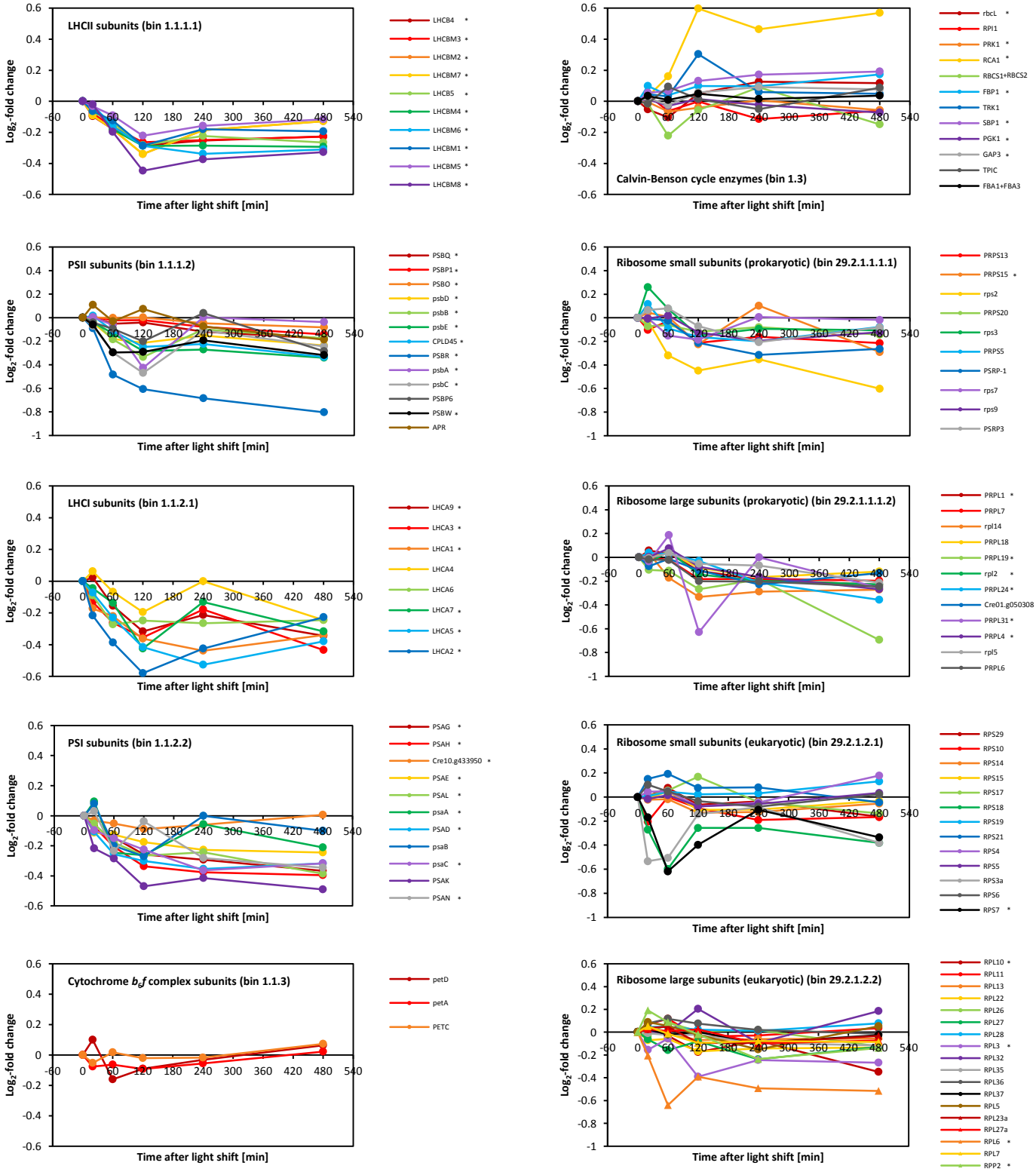

Supplemental Figure 9. Protein Levels in *C. reinhardtii* CC-1690 Cells During the Light Shift Experiment within the Functional Categories "Light Reaction", "CBC" and "Ribosomes".

Kinetics of individual proteins of selected functional categories based on MapMan ontology (bin number indicated in parentheses). Central tendencies are shown in Figure 4. Asterisks mark significantly changed proteins groups (p-value<0.05). To allow good visualization of all CBC proteins, data for FBA1 and FBA3 were combined as FBA1 is a minor component of aldolase activity (Blaby et al. 2013; see text and Supplemental Table 1). Asterisks indicate proteins that change significantly (ANOVA p-value<0.05, after p-value correction for multiple sampling by Benjamini-Hochberg). For further details of analyses see Methods.

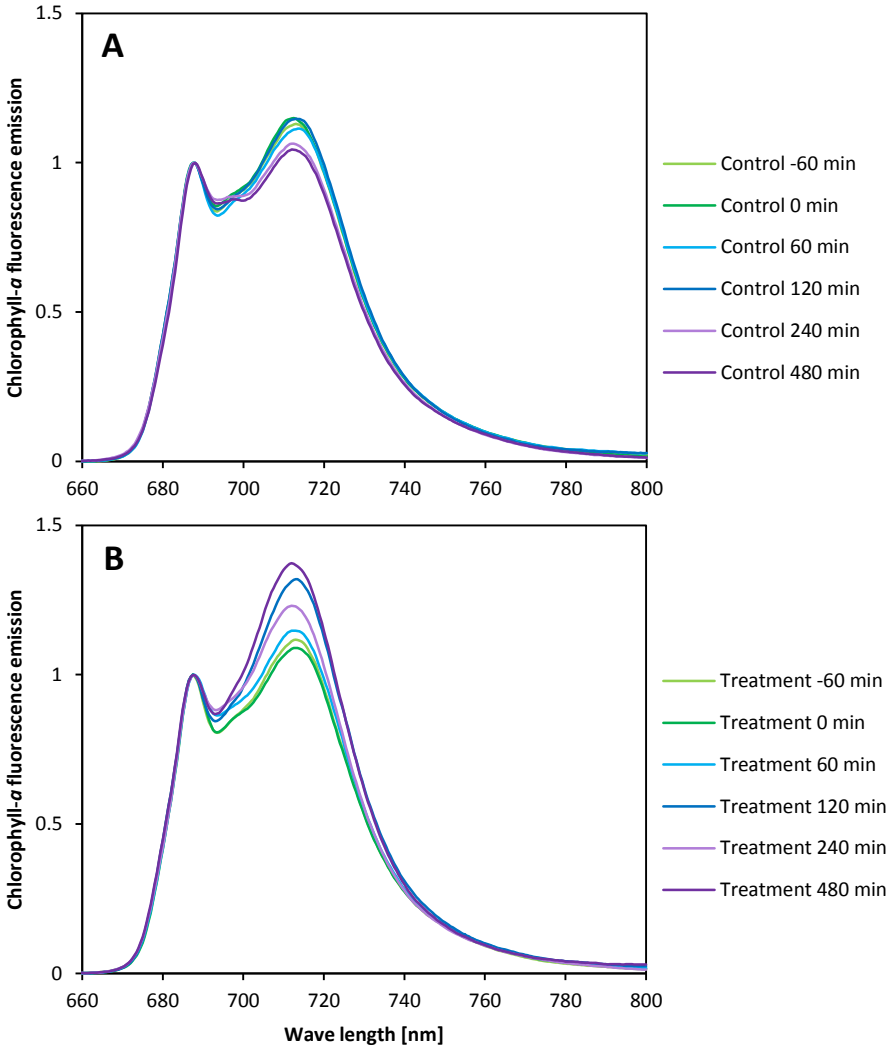

Supplemental Figure 10. 77K Fluorescence Emission Spectra during Light Shift.

For comparability of the different emission signals, the maximum fluorescence emission of PSII at 687 nm wavelength was normalized to one.
(A) In the control conditions , *C. reinhardtii* CC-1690 cells were exposed to a light intensity of 41 µmol photons*m^{-2}*s^{-1} for the course of the experiment. A 77K fluorescence emission spectrum was measured at -60 min, 0 min, 60 min, 120 min, 240 min and 480 min during the time course.
(B) In the treatment conditions, light intensity was shifted from 41 to 145 µmol photons*m^{-2}*s^{-1} at time point zero. A 77K fluorescence emission spectrum was measured one hour before the light shift (-60min), just before the light shift (0 min) and 60 min, 120 min, 240 min and 480 min after the light shift.

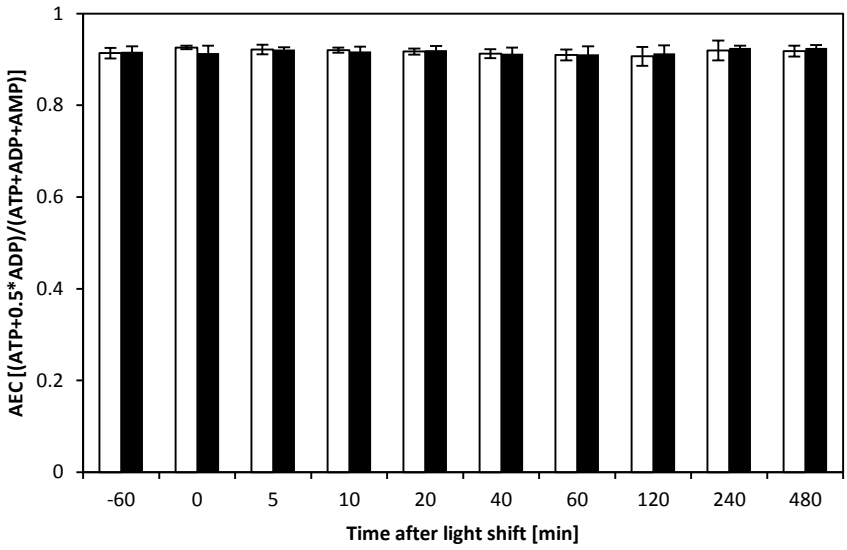

Supplemental Figure 11. Adenylate Energy Charge (AEC) during Light Shift.

From ATP measured spectrophotometrically and ADP and AMP measured via LC-MS/MS in *C. reinhardtii* CC-1690 cells, the AEC was calculated for each measured time point in the control samples (white bars), where light was kept at 41 µmol photons*m^{-2}*s^{-1}, and the treatment samples (black bars), where light was shifted to 145 µmol photons*m^{-2}*s^{-1} at time point zero (n = 4 ± SD).

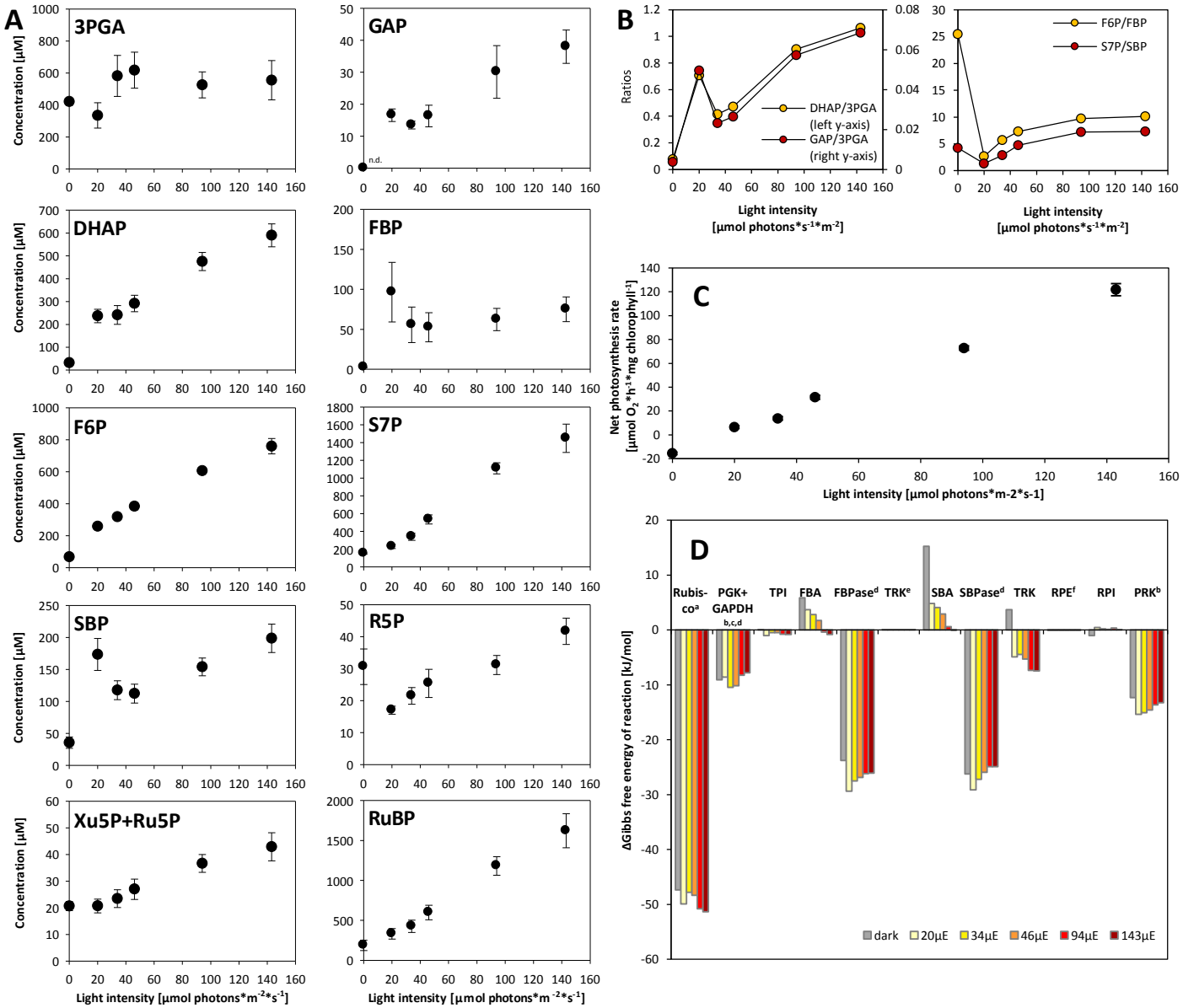

Supplemental Figure 12. CBC Intermediate Levels Change with Increasing Light Intensity.

C. reinhardtii CC-1690 cells were grown in a bioreactor at 24°C, 5% CO_2 and 46 µmol photons*m^{-2}*s^{-1}. Before harvesting and measurement cells were exposed for one hour to darkness or to the indicated light intensities.

(A) CBC intermediate levels in the dark and five different light intensities were measured by LC-MS/MS (n = 8, ± SD).

(B) Metabolite ratios for selected CBC intermediates based on metabolite levels shown in A.

(C) Net photosynthesis rates in *Chlamydomonas* cells were measured after the addition of 10 mM sodium bicarbonate at the corresponding light intensities in an external closed cuvette using an optical oxygen sensor (n = 4, ± SD).

(D) Gibbs free energy of reaction (Δ_rG) of Calvin-Benson cycle enzymes. For calculations, standard free energies ($\Delta_rG^{0'}$) from Bassham and Krause (1969) and the formula $\Delta_rG = \Delta_rG^{0'} + R*T*\ln(MAR)$ were used, where the mass action ratio (MAR) is the reaction quotient that was calculated based on the CBC intermediate levels shown in A. The following assumption were made: [a] $[CO_2]$ under 5% CO_2 conditions was assumed to be 0.202M. [b] ATP/ADP=3 (light), ATP/ADP=0.5 (dark) (Gardestrom and Wigge, 1988), [c] NADPH/$NADP^+$=1 (light), NADPH/$NADP^+$=0.5 (dark) (Heineke et al., 1991), [d] $[P_i]$=0.002M (Pratt et al., 2009). [e] The first TRK reaction was assumed to be at equilibrium to estimate the in vivo concentration of E4P. The fact that Δ_rG of SBA is also close to zero in the light supports the assumption that the first TRK and SBA catalysed reactions are close to equilibrium and either reaction could have been used to estimate E4P concentration, with approximately the same result. This was not the case for cells exposed to dark. The TRK and SBA reaction are likely not at equilibrium in the dark and E4P estimation is difficult. [f] The RPE reaction was assumed to be at equilibrium to estimate individual levels of X5P and Ru5P, which are stereoisomers and not distinguishable with LS-MS/MS. The Δ_rG of RPI being close to zero supports this assumption.

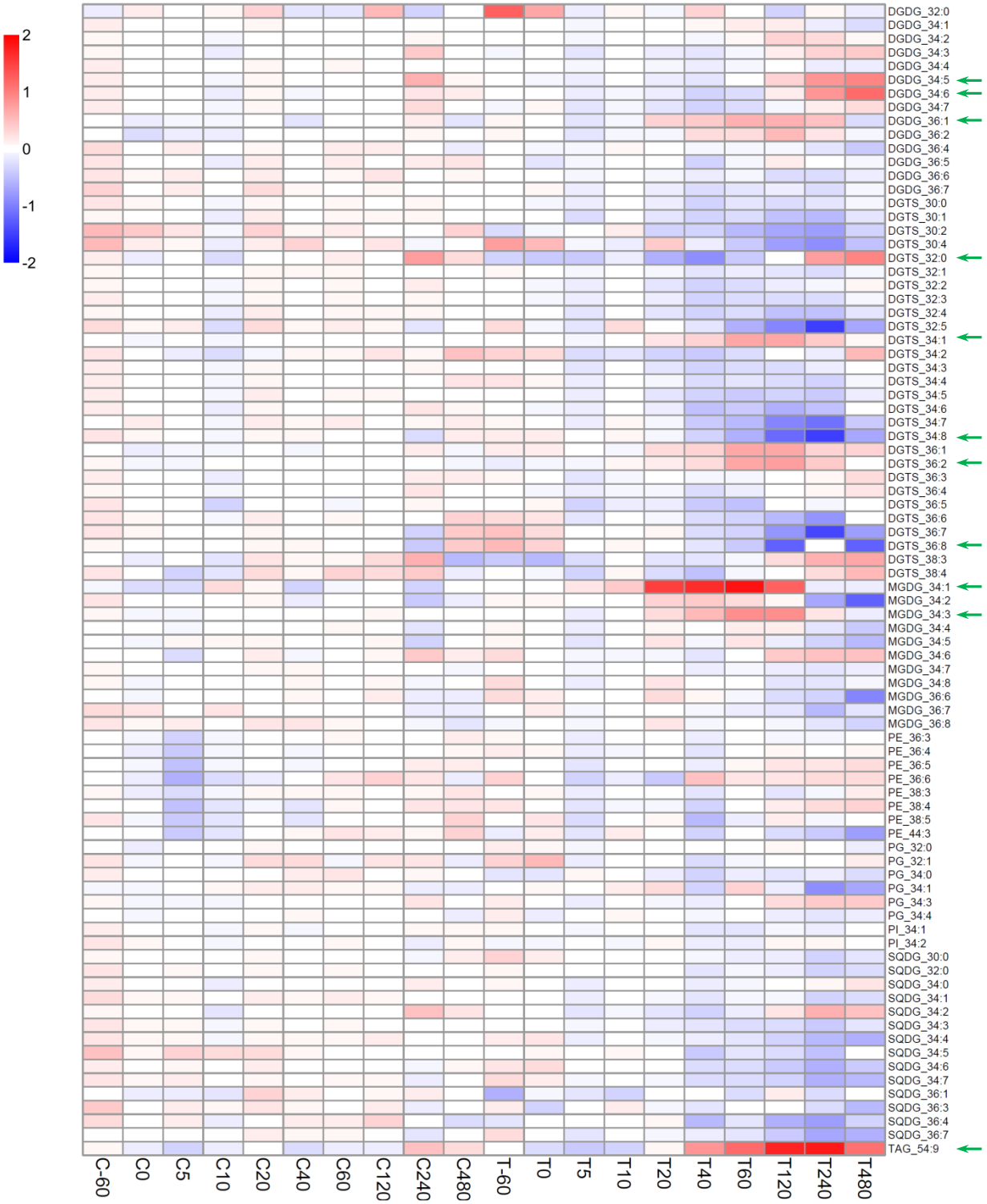

Supplemental Figure 13. Heatmap of Lipid Levels during Light Shift in *C. reinhardtii* CC-1690 Cells.

Log_2-normalized data are shown where for each time point the value was centred to the median of the corresponding lipid. Color key indicates lipid accumulation value, blue: lowest, red: highest. Arrows indicate lipids that change significantly (ANOVA p-value<0.05, after p-value correction for multiple sampling by Benjamini-Hochberg).

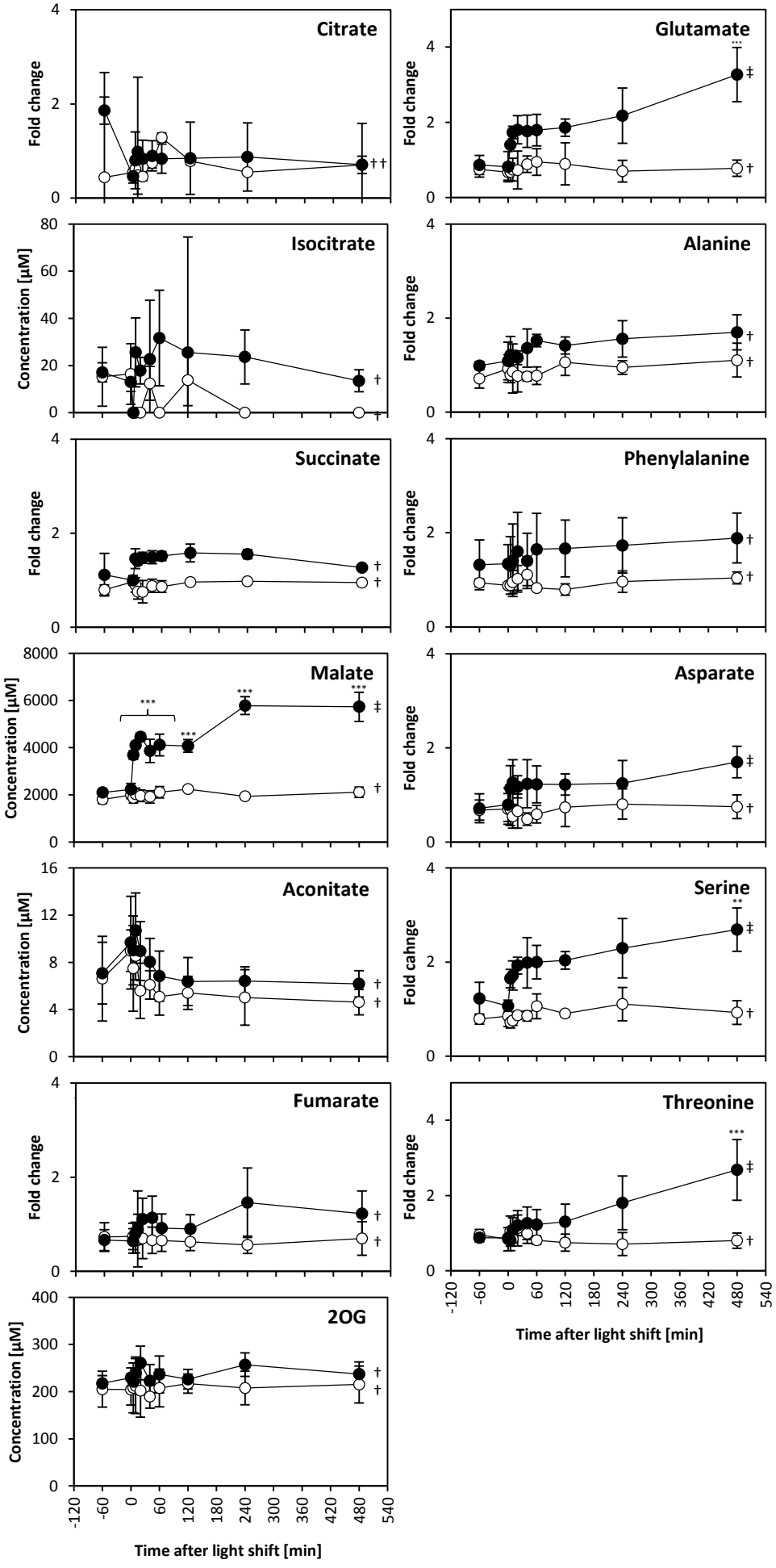

Supplemental Figure 14. Amino Acids and Organic Acids.

C. reinhardtii CC1690 cells were grown in a bioreactor at 24°C, 5% CO_2 and 41 µmol photons*m^{-2}*s^{-1} (open circles) or shifted to 145 µmol photons*m^{-2}*s^{-1} at time point zero (filled circles). Metabolites were separated and detected by LC-MS/MS (isocitrate, malate, aconitate, 2OG) (n = 4 ± SD). Metabolite levels are given as concentrations (µM; see Methods). Citrate, succinate, fumarate, glutamate, alanine, phenylalanine, aspartate, serine and threonine were separated and detected by GC-MS (n = 3 ± SD) and given in fold-changes normalized to all reference time points (see Methods). Pairwise t-test between control and treatment was done and p-value correction for multiple sampling by Bonferroni correction (one asterisk, $p < 0.05$; two asterisks, $p < 0.01$; three asterisks, $p < 0.001$). ANOVA analysis was done and p-value correction for multiple sampling by Benjamini-Hochberg correction (dagger, $p > 0.05$; double dagger, $p < 0.05$). Graphs are based on data given in Supplemental Dataset 1.

A

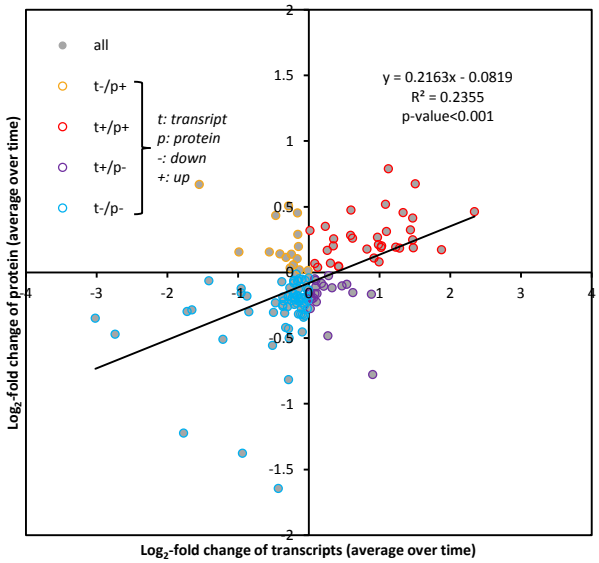

B

Bin	Bin name	n	Pearson correlation coefficient	R^2	p-value
11.1	lipid metabolism.FA synthesis and FA elongation	4	0.991	0.983	<0.001*
9.09	mitochondrial electron transport / ATP synthesis.F1-ATPase	5	0.947	0.896	0.004*
13.1	amino acid metabolism.synthesis	7	0.889	0.791	0.003
29.6.2	protein.folding	6	0.868	0.753	0.013*
1.1.1.2	PS.lightreaction.photosystem II.PSII polypeptide subunits	5	0.790	0.623	0.076
35.2	not assigned.unknown	10	0.756	0.572	0.008
29.2.1.1.1	protein.synthesis.ribosomal protein.prokaryotic.chloroplast	7	-0.604	0.365	0.134
1.3	PS.calvin cycle	6	-0.603	0.364	0.181
1.1.1.01	PS.lightreaction.photosystem II.LHC-II	6	-0.569	0.324	0.215
29.2.1	protein.synthesis.ribosomal protein	6	-0.499	0.249	0.293
1.1.2.2	PS.lightreaction.photosystem I.PSI polypeptide subunits	6	-0.394	0.155	0.424
31.6.1.10	cell.motility.eukaryotes.flagellar associated proteins	4	0.225	0.051	0.760
28.1.3	DNA.synthesis/chromatin structure.histone	5	-0.114	0.013	0.851

C

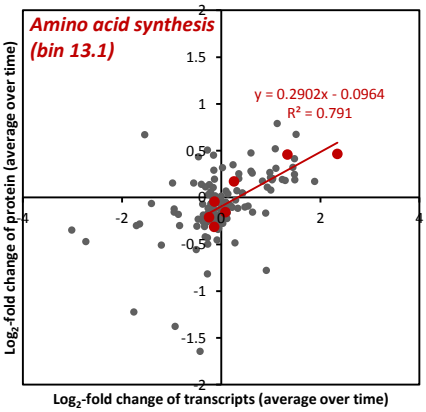

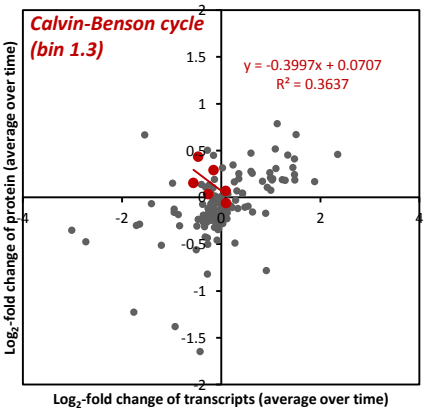

D

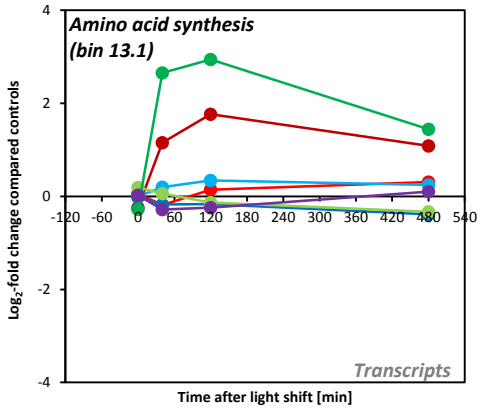

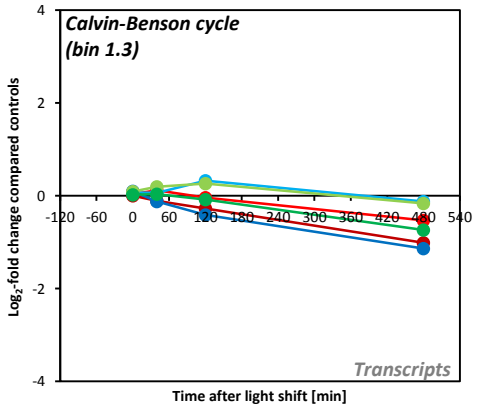

E

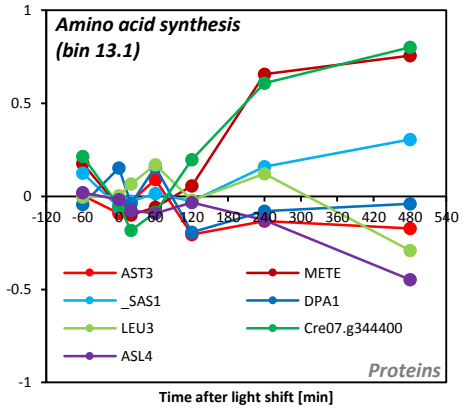

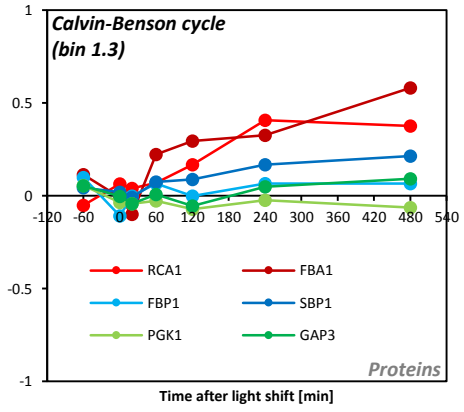

Supplemental Figure 15. Correlation between Average Changes in Transcript and Protein Group Levels.

C. reinhardtii CC-1690 cells were grown in a bioreactor at 24°C, 5% CO_2 and 41 µmol photons*m^{-2}*s^{-1} and shifted to 145 µmol photons*m^{-2}*s^{-1} at time point zero. Levels of transcripts and protein groups were measured during the light shift as described in Methods. Average log_2-fold changes of samples exposed to higher light and changing significantly (ANOVA, p-value<0.05 after p-value correction by Benjamini-Hochberg method) are plotted against each other **(A)**. Pearson correlation coefficients between average changes of transcripts and protein groups were calculated for individual MapMan bins with a minimum of four members (**B**; red, positive correlation; blue, negative correlation; asterisk, significant correlations driven by single members). For two of these bins, details are shown in C-E.

(C) The average of log_2-fold change over time of transcripts is plotted versus the average log_2-fold change of the different protein groups and shown in grey as in A. In red, data for two MapMan bin is highlighted (bin 13.1 and 1.3).

(D) The time course of the transcript levels belonging to the MapMan bins 13.1 and 1.3, respectively, are shown.

(E) The time course of the protein groups belonging to the MapMan bins 13.1 and 1.3, respectively, are shown.

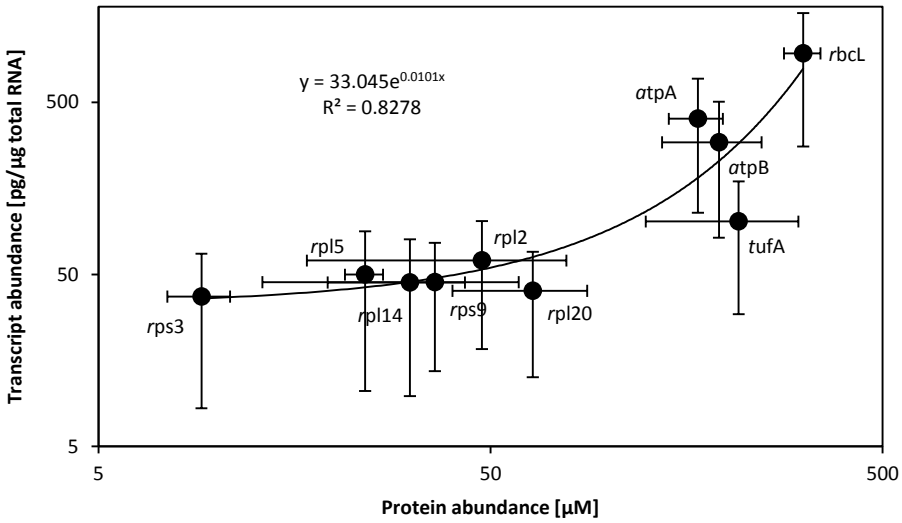

Supplemental Figure 16. Correlation between Protein Levels and Transcript Levels for Plastid-encoded Genes in *C. reinhardtii* CC-1690 Cells.

Proteins and transcripts were quantified by the emPAI method (see Supplemental Table 1 and Methods) and microarray analysis with normalisation to synthetic spike-in RNAs (Kahlau and Bock, 2008), respectively. The ten plastid-encoded proteins which were quantified by emPAI showed a significant correlation ($R^2 = 0.83$, $p = 0.0002$) with their respective transcript levels (n = 3 ± SD).

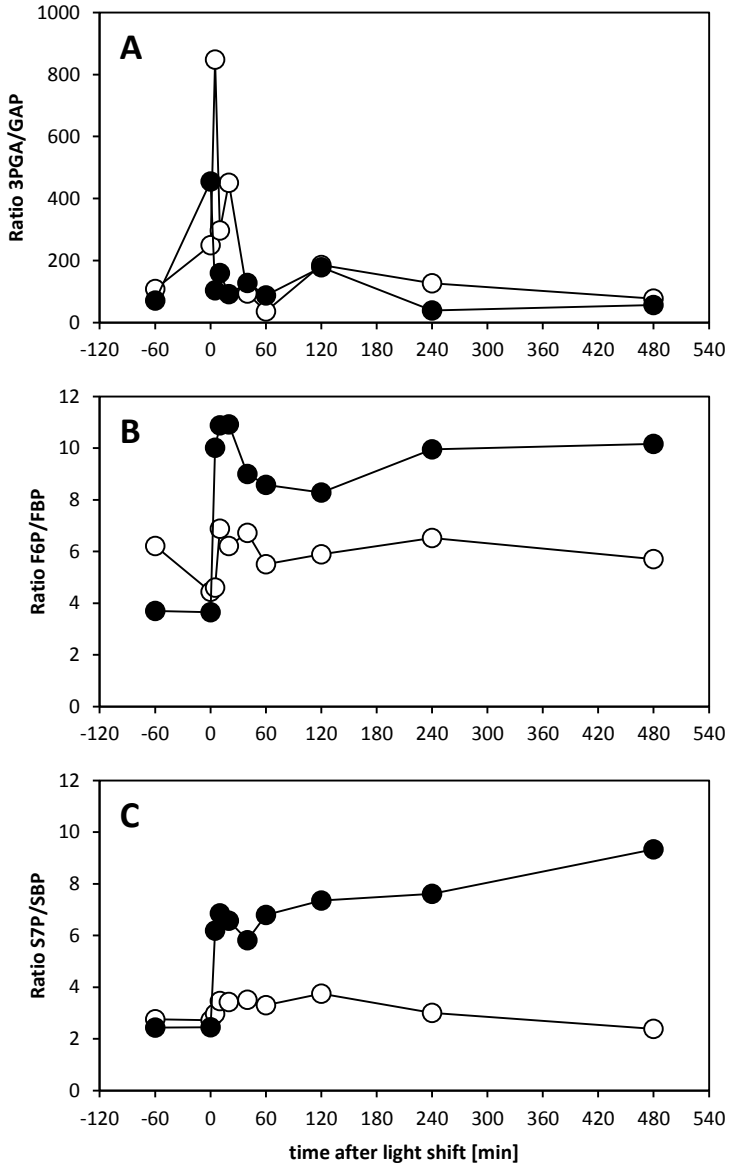

Supplemental Figure 17. Calculated Metabolite Ratios.

C. reinhardtii CC-1690 cells were grown in a bioreactor at 24°C, 5% CO_2 and 41 µmol photons*m^{-2}*s^{-1}. At time point zero the light was either kept at the initial light intensity (open circles) or shifted to 145 µmol photons*m^{-2}*s^{-1} (filled circles) at time point zero. Based on the metabolite concentrations shown in Figure 6 and Supplemental Dataset 1, the ratios of 3PGA/GAP **(A)**, F6P/FBP **(B)** and S7P/SBP **(C)** were calculated from the average metabolite levels (n = 4).

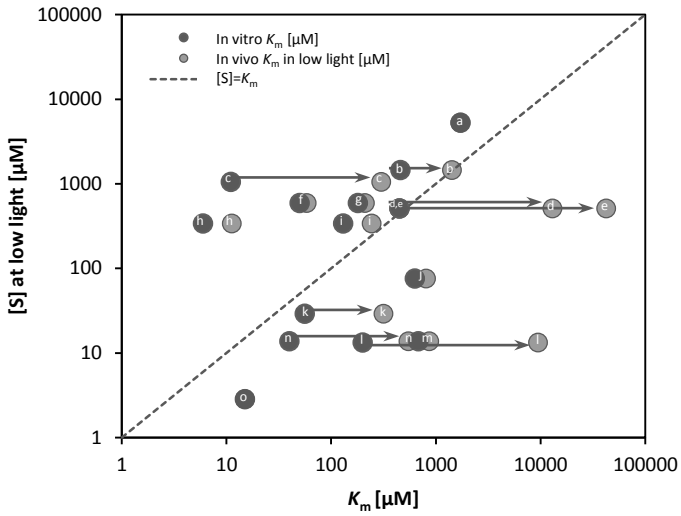

Supplemental Figure 18. In Vitro and in Vivo K_m-values versus Substrate Concentrations [S].

The substrate levels at low light of CBC reactions in *C. reinhardtii* CC-1690 cells (shown in Figure 6) are plotted against in vitro K_m (dark grey) (literature values, for details see Supplemental Table 6) and in vivo K_m (light grey) calculated based on substrate saturation curves (shown in Figure 11). In Figure 12, an equal plot with substrate levels 20 min after the light shift is shown. Arrows indicate >2-fold increases between in vitro and in vivo K_m-values. Enzymes with their substrate in parentheses: [a] PGK (3PGA), [b] TRK (S7P), [c] Rubisco (RuBP), [d] FBA (DHAP), [e] SBA (DHAP), [f] oxidized SBPase (SBP), [g] reduced SBPase (SBP), [h] oxidized FBPase (FBP), [i] reduced FBPase (FBP), [j] RPI (R5P), [k] PRK (Ru5P), [l] SBA (E4P), [m] TPI (GAP), [n] FBA (GAP), [o] GAPDH (BPGA).

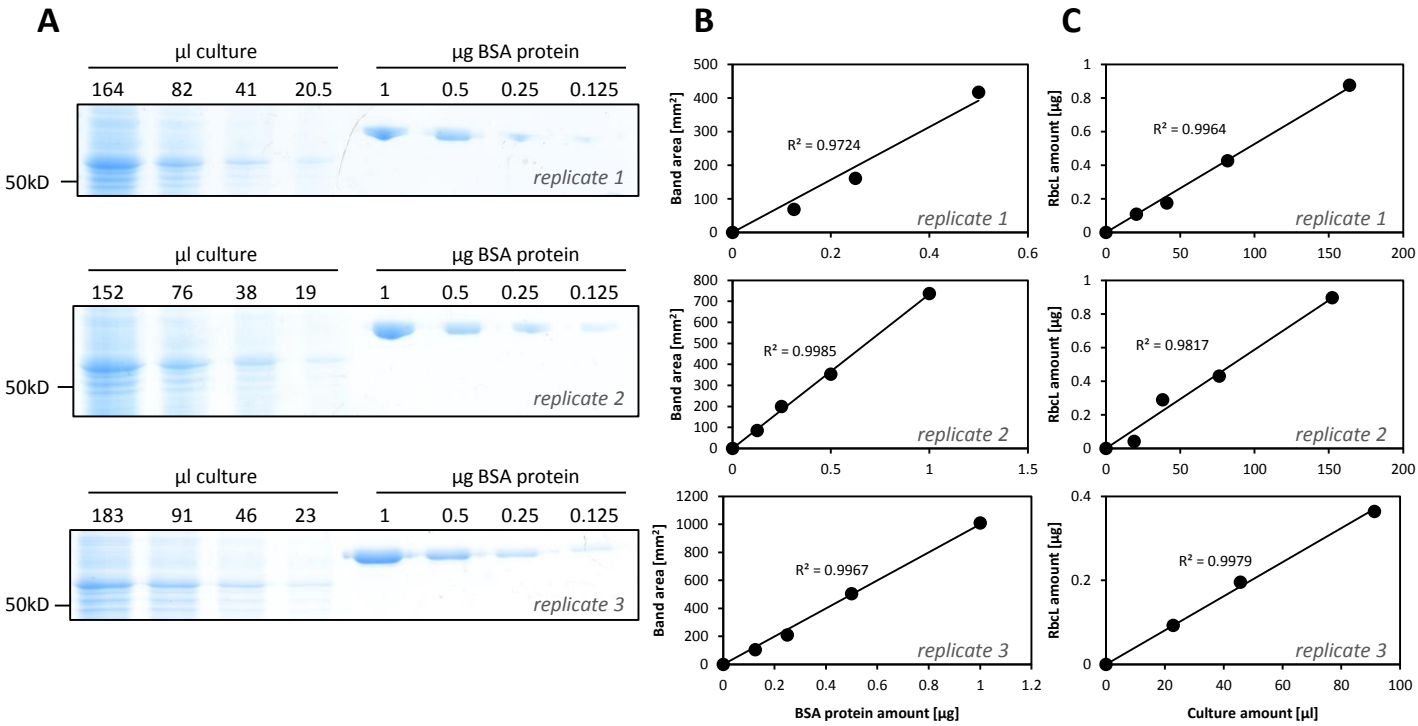

Supplemental Figure 19. Amount of RbcL Protein in *C. reinhardtii* Cells.

(A) Three replicates of Coomassie-stained SDS-gels with 4 different concentrations of cell culture and BSA protein standard (cell density of the cultures from top to bottom were: 1052, 1052 and 969 nl total cell volume*ml^{-1}).
(B) Three replicates of standard curves plotting BSA protein amounts versus band area calculated by the Quantity One 1-D Analysis Software after background subtraction.
(C) Three replicates of RbcL amounts per µl culture used for the calculation of RbcL amount after background subtraction. The µg RbcL/µl cell culture were then transformed to RbcL concentration [µM] considering the measured cell volume per ml culture, the volume of the chloroplast, the absolute weight of RbcL and the Avogadro constant.

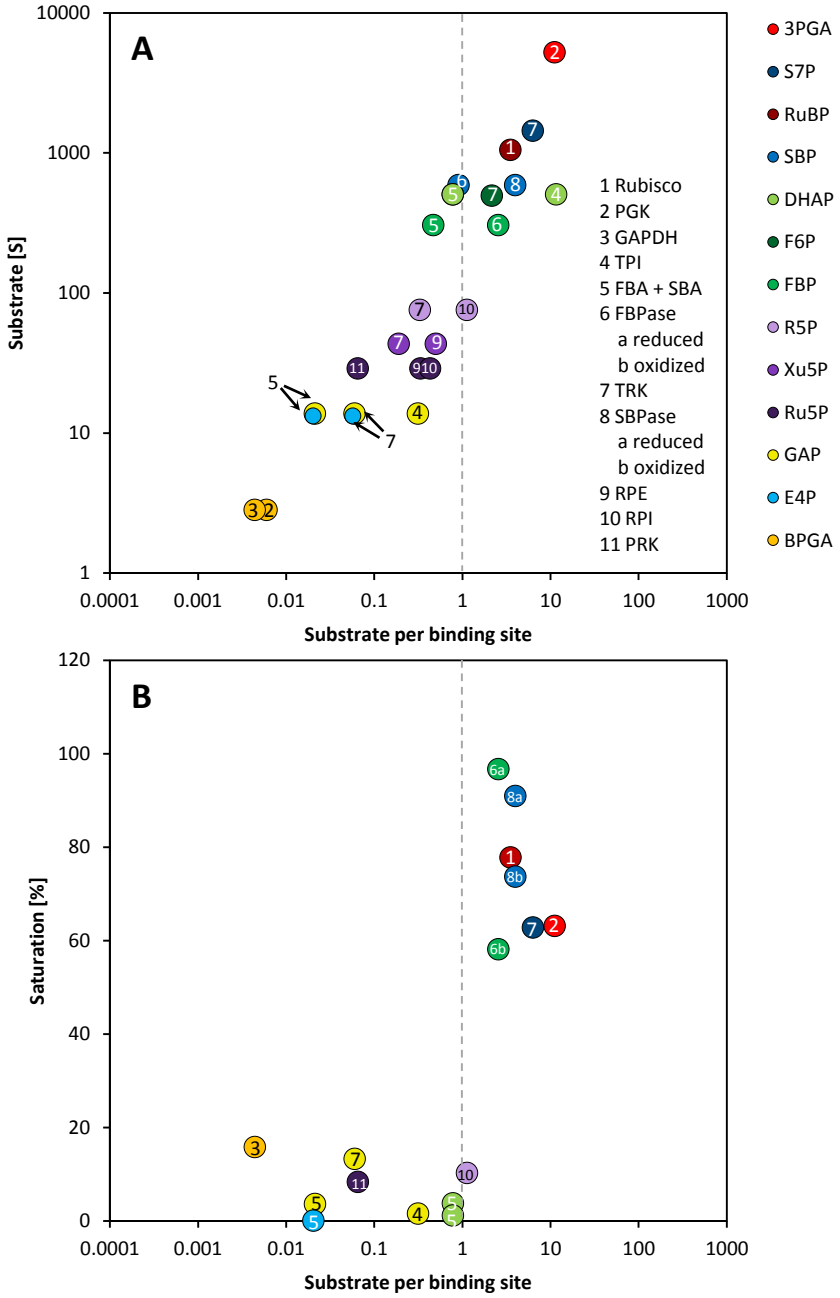

Supplemental Figure 20. Substrate per Binding Sites versus Substrate Concentrations (A) and Enzyme Saturation (B) of CBC Enzymes.

Substrates of CBC reactions were measured via LC-MS/MS and are shown in Figure 6. Binding sites of CBC enzymes were calculates based on proteomics data via the emPAI as described in text, Supplemental Table 1 and Methods.
(A) Substrate per binding site of CBC reactions plotted against the substrate level before the light intensity was increased from 41 to 145 µmol photons*m^{-2}*s^{-1} (time point zero).
(B) Substrate per binding site of CBC reactions plotted against the degree of saturation according to the saturation curves shown in Figure 11, before the light intensity was increased from 41 to 145 µmol photons*m^{-2}*s^{-1} (time point zero). For a similar plot 20 min after the light shift, see Figure 13.

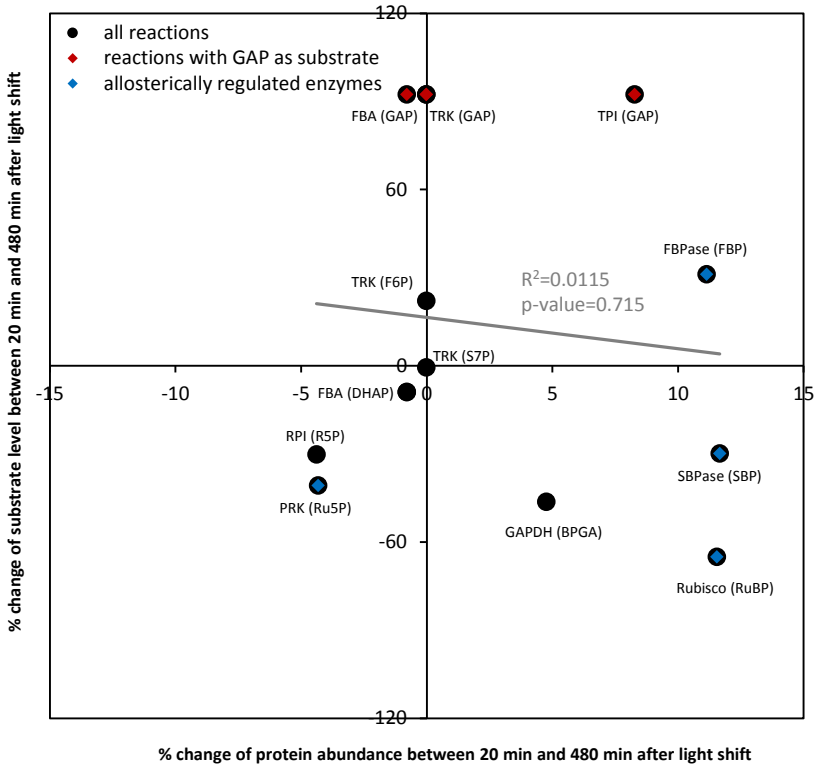

Supplemental Figure 21. Percentage Change for Enzyme-substrate Pairs of the CBC between 20 min and 480 min After the Light Shift Applied to *C. reinhardtii* CC-1690 Cells.

Supplemental Table 1. Binding Site Concentration of CBC Enzymes Based on emPAI Analysis of Proteomics Data.

Binding site concentrations at the lower light intensity were calculated by the emPAI and normalized to measured amounts of Rubisco (for details see text and Methods). For comparison, substrate data of time point zero at the lower light intensity and 20 min after the light shift are shown in column four and five, respectively. In column six and seven the ratio between substrate and binding site was calculated for time point zero and 20 min after the light shift, respectively.
[a]Of the aldolase encoding genes, *FBA1* and *FBA3* were suggested to be localized in the chloroplast and *FBA3* transcript was shown to be higher expressed in *C. reinhardtii* strain CC-4249 (Blaby et al., 2013). In this study, based on the amount of protein calculated via the emPAI-value, FBA3 protein was found to be >30-fold more abundant than FBA1. The binding site concentration for the aldolase reaction (FBA and SBA, two reactions catalysed by the same enzyme) is the sum of the calculated abundance of FBA1 and FBA3.

			Substrate [µM]		Substrate per binding site	
Enzyme name	**Binding site [µM]**	**Substrate**	**before light shift**	**20 min after light shift**	**before light shift**	**20 min after light shift**
Rubisco	304.5 ± 32.6	RuBP	1057.5	5189.2	3.5	17.0
PGK	477.2 ± 54.5	3PGA	5261.3	7447.1	11.0	15.6
		BPGA	2.8	4.0	0.0	0.0
GAPDH	651.5 ± 189.0	BPGA	2.8	4.0	0.0	0.0
TPI	44.3 ± 10.6	GAP	13.8	32.1	0.3	0.7
		DHAP	509.4	1098.2	11.5	24.8
FBA[a]	658.5 ± 99.7	GAP	13.8	32.1	0.0	0.0
		DHAP	509.4	1098.2	0.8	1.7
		FBP	306.1	257.2	0.5	0.4
FBPase	121.0 ± 13.2	FBP	306.1	257.2	2.5	2.1
TRK	232.2 ± 47.0	F6P	498.9	1255.0	2.1	5.4
		GAP	13.8	32.1	0.1	0.1
SBA[a]	658.5 ± 99.7	E4P	13.3	39.7	0.0	0.1
		DHAP	509.4	1098,2	0.8	1.7
		SBP	591.0	919.2	0.9	1.4
SBPase	149.6 ± 29.8	SBP	591.0	919.2	3.9	6.1
TRK	232.2 ± 47.0	S7P	1450.6	6048.2	6.2	26.0
		GAP	13.8	32.1	0.1	0.1
		R5P	76.1	133.7	0.3	0.6
		Xu5P	43.7	85.1	0.2	0.4
RPE	87.7 ± 39.8	Xu5P	43.7	85,1	0.5	1.0
		Ru5P	29.1	56.8	0.3	0.6
RPI	68.1 ± 14.8	R5P	76.1	133.7	1.1	2.0
		Ru5P	29.1	56.8	0.4	0.8
PRK	451.3 ± 93.8	Ru5P	29.1	56.8	0.1	0.1

Supplemental Table 2. The Rate Equations of the CBC Reactions.

Rate equations according to Methods and Fridlyand and Scheibe (1999) used for calculation of substrate saturation curves (shown in Figure 11) together with the K_m and K_I values information of Supplemental Table 3 and metabolite amounts shown in Figure 6 and Supplemental Dataset 1.

Enzyme	Rate equation
Rubisco	$v_1 = \frac{[RuBP]*W_C*\min\left(1,\frac{[RuBP]}{[E_t]}\right)}{[RuBP]+K_{m13}\left(1+\frac{[3PGA]}{K_{I11}}+\frac{[FBP]}{K_{I12}}+\frac{[SBP]}{K_{I13}}+\frac{[P_i]}{K_{I14}}+\frac{[NADPH]}{K_{I15}}\right)}$ $W_C = V_{Cmax} * \frac{[CO_2]}{[CO_2]+K_{m11}\left(1+\frac{[O_2]}{K_{m12}}\right)}$
PGK	$\frac{v_2}{V_{max}} = \frac{[3PGA]*[ATP]-\frac{[BPGA]*[ADP]}{K_{E2}}}{K_{m21}*K_{m22}*\left(1+\frac{[3PGA]}{K_{m71}}+\frac{[ATP]}{K_{m72}}+\frac{[BPGA]}{K_{m73}}+\frac{[ADP]}{K_{m74}}+\frac{[3PGA]*[ATP]}{K_{m71}*K_{m72}}+\frac{[BPGA]*[ADP]}{K_{m73}*K_{m74}}\right)}$
GAPDH	$\frac{v_3}{V_{max}} = \frac{[BPGA]*[NADPH]}{([BPGA]+K_{m31})*([NADPH+K_{m32})}$
TPI	$\frac{v_4}{V_{max}} = \frac{[GAP]-\frac{[DHAP]}{K_{E4}}}{K_{m41}*K_{m42}*\left(1+\frac{[GAP]}{K_{m41}}+\frac{[DHAP]}{K_{m42}}\right)}$
FBA	$\frac{v_5}{V_{max}} = \frac{[GAP]*[DHAP]-\frac{[FBP]}{K_{E5}}}{K_{m51}*K_{m52}*\left(1+\frac{[GAP]}{K_{m51}}+\frac{[DHAP]}{K_{m52}}+\frac{[GAP]*[DHAP]}{K_{m51}*K_{m52}}+\frac{[FBP]}{K_{m53}}\right)}$
FBPase	$\frac{v_6}{V_{max}} = \frac{[FBP]}{[FBP]+K_{m61}*\left(1+\frac{[F6P]}{K_{I61}}+\frac{[P_i]}{K_{I62}}\right)}$
SBA	$\frac{v_7}{V_{max}} = \frac{[E4P]*[DHAP]-\frac{[SBP]}{K_{E7}}}{K_{m71}*K_{m72}*\left(1+\frac{[E4P]}{K_{m71}}+\frac{[DHAP]}{K_{m72}}+\frac{[E4P]*[DHAP]}{K_{m71}*K_{m72}}+\frac{[SBP]}{K_{m73}}\right)}$
SBPase	$\frac{v_8}{V_{max}} = \frac{[SBP]}{[SBP]+K_{m81}*\left(1+\frac{[P_i]}{K_{I81}}\right)}$
TRK	$\frac{v_9}{V_{max}} = \frac{[S7P]*[GAP]-\frac{[R5P]*[Xu5P]}{K_{E9}}}{K_{m91}*K_{m92}*\left(1+\frac{[S7P]}{K_{m91}}+\frac{[GAP]}{K_{m92}}+\frac{[R5P]}{K_{m93}}+\frac{[Xu5P]}{K_{m94}}+\frac{[S7P]*[GAP]}{K_{m91}*K_{m92}}+\frac{[R5P]*[Xu5P]}{K_{m93}*K_{m94}}\right)}$
RPI	$\frac{v_{10}}{V_{max}} = \frac{[R5P]-\frac{[Ru5P]}{K_{E10}}}{K_{m101}*\left(1+\frac{[R5P]}{K_{m101}}+\frac{[Ru5P]}{K_{m102}}\right)}$
PRK	$\frac{v_{11}}{V_{max}} = \frac{[Ru5P]*[ATP]}{\left([Ru5P]+K_{m111}*\left(1+\frac{[3PGA]}{K_{I111}}+\frac{[RuBP]}{K_{I112}}+\frac{[P_i]}{K_{I113}}\right)\right)*\left([ATP]+K_{m112}*\left(1+\frac{[ADP]}{K_{I114}}\right)\right)}$

Supplemental Table 3. K_m and K_I Values of Substrates and Inhibitors from CBC Enzymes.

K_m and K_I from literature that were used for calculation of substrate saturation curves (shown in Figure 11) together with the rate equations given in Supplemental Table 2 and metabolite amounts shown in Figure 6 or Supplemental Dataset 1.

Enzyme	EC Number	Reaction	Substrate or inhibitor	Parameter	Value [mM]	Organism	Reference
Rubisco	4.1.1.39	RuBP+CO_2→3PGA+3PGA	CO_2	K_{m11}	0.033	*Chlamydomonas reinhardtii*	Spreitzer et al. (1995)
			O_2	K_{m12}	0.381	*Chlamydomonas reinhardtii*	Spreitzer et al. (1995)
			RuBP	K_{m13}	0.011	*Chlamydomonas reinhardtii*	Spreitzer et al. (1995)
			3PGA	K_{I11}	0.84	*Spinacia oleaceae*	Badger and Lorimer (1981)
			FBP	K_{I12}	0.04	*Spinacia oleaceae*	Badger and Lorimer (1981)
			SBP	K_{I13}	0.075	*Spinacia oleaceae*	Badger and Lorimer (1981)
			P_i	K_{I14}	0.9	*Spinacia oleaceae*	Badger and Lorimer (1981)
			NADPH	K_{I15}	0.07	*Spinacia oleaceae*	Badger and Lorimer (1981)
PG*K*	2.7.2.3	3PGA+ATP↔BPGA+ADP	3PGA	K_{m21}	1.72	*Spinacia oleaceae*	Köpke-Secundo et al. (1990)
			ATP	K_{m22}	0.39	*Spinacia oleaceae*	Köpke-Secundo et al. (1990)
			BPGA	K_{m23}	0.004	*Spinacia oleaceae*	Trost et al. (1993)
			ADP	K_{m24}	0.27	*Homo sapiens*	Varga et al. (2008)
				K_{E2}	$7.6*10^{-4}$	*Estimated*	Zhu et al. (2007)
GAPDH	1.2.1.13	BPGA+NADPH→GAP+$NADP^+$+P_i	3PGA	K_{m31}	0.015	*Spinacia oleaceae*	Sparla et al. (2005)
			ATP	K_{m32}	0.018	*Chlamydomonas reinhardtii*	Graciet et al. (2003)
TPI	5.3.1.1	GAP↔DHAP	GAP	K_{m41}	0.68	*Spinacia oleaceae*	Harris and *K*oniger (1997)
			DHAP	K_{m42}	2.5	*Spinacia oleaceae*	Harris and Koniger (1997)
				K_{E4}	22.2	*Chlorella pyrenoidosa*	Bassham and Krause (1969)
FBA	4.1.2.13	GAP+DHAP↔FBP	GAP	K_{m51}	0.04	*Spinacia oleaceae*	Iwaki et al. (1991)
			DHAP	K_{m52}	0.45	*Spinacia oleaceae*	Iwaki et al. (1991)
			FBP	K_{m53}	0.0091	*Pisum sativum*	Schnarrenberger et al. (1989)
				K_{E5}	7.1	*Chlorella pyrenoidosa*	Bassham and Krause (1969)
FBPase	3.1.3.11	FBP→F6P+P_i	FBP	K_{m61}(red)	0.06	*Spinacia oleaceae*	Cadet and Meunier (1988)
			FBP	K_{m61}(ox)	0.13	*Spinacia oleaceae*	Cadet and Meunier (1988)
			F6P	K_{I61}	0.7	*Spinacia oleaceae*	Gardemann et al. (1986)
			P_i	K_{I62}	12	*Pisum sativum*	Charles and Halliwell (1981)
SBA	4.1.2.13	E4P+DHAP↔SBP	E4P	K_{m71}	0.2	*Estimated*	Zhu et al. (2007)
			DHAP	K_{m72}	0.45	*Spinacia oleaceae*	Iwaki et al. (1991)
			SBP	K_{m73}	0.006	*Daucus carota*	Moorhead and Planxton (1990)
SBPase	3.1.3.37	SBP→S7P+P_i	SBP	K_{m81}(red)	0.05	*Spinacia oleaceae*	Cadet and Meunier (1988)
			SBP	K_{m81}(ox)	0.18	*Spinacia oleaceae*	Cadet and Meunier (1988)
			P_i	K_{I81}	12000	*Triticum aestivum*	Woodrow et al. (1983)
TRK	2.2.1.1	S7P+GAP↔R5P+Ru5P	S7P	K_{m91}	0.46	*Dictyostelium discoideum*	Albe (1991)
			GAP	K_{m92}	0.072	*Dictyostelium discoideum*	Albe (1991)
			R5P	K_{m93}	0.33	*Spinacia oleaceae*	Teige et al. (1998)
			Xu5P	K_{m94}	0.067	*Spinacia oleaceae*	Teige et al. (1998)
				K_{E9}	0.847	*Chlorella pyrenoidosa*	Bassham and Krause (1969)
RPI	5.3.1.6	R5P↔Ru5P	R5P	K_{m101}	0.63	*Spinacia oleaceae*	Jung et al. (2000)
			Ru5P	K_{m102}	0.66	*Pisum sativum*	Skrukrud et al. (1991)
				K_{E10}	0.4	*Chlorella pyrenoidosa*	Bassham and Krause (1969)
PRK	2.1.7.19	Ru5P+ATP→RuBP+ADP	Ru5P	K_{m111}	0.056	*Chlamydomonas reinhardtii*	Roesler et al. (1990)
			ATP	K_{m112}	0.059	*Spinacia oleaceae*	Gardemann et al. (1983)
			3PGA	K_{I111}	2	*Spinacia oleaceae*	Gardemann et al. (1983)
			RuBP	K_{I112}	0.7	*Spinacia oleaceae*	Gardemann et al. (1983)
			P_i	K_{I113}	4	*Spinacia oleaceae*	Gardemann et al. (1983)
			ADP	K_{I114}	0.04	*Spinacia oleaceae*	Gardemann et al. (1983)

Supplemental Table 4. Binding Site Concentration of CBC Enzymes Based on emPAI Analysis of Proteomics Data with Two Different Methods.

Method A: The relative abundance calculated by the emPAI (see Methods) was normed on total protein.
Method B: The relative abundance calculated by the emPAI (see Methods) was normed on total protein after correcting the latter for the fraction of the total annotated *C. reinhardtii* proteins that were detected in our analysis (n = 4) (i.e. after multiplying total protein by number of detected proteins/number of annotated proteins= 767/17038). [a]See legend of Supplemental Table 1.

Enzyme name	Method A: binding site [µM]	Method B: binding site [µM]
Rubisco	1006 ± 108	45.2 ± 4.8
PGK	1577 ± 180	70.8 ± 8.1
GAPDH	2153 ± 625	96.7 ± 28.0
TPI	146 ± 35	6.6 ± 1.6
[a]FBA	2176 ± 330	97.7 ± 14.8
FBPase	400 ± 44	18.0 ± 2.0
TRK	767 ± 155	34.4 ± 7.0
[a]SBA	2176 ± 330	97.7 ± 14.8
SBPase	494 ± 99	22.2 ± 4.4
TRK	767 ± 155	34.4 ± 7.0
RPE	290 ± 132	13.0 ± 5.9
RPI	225 ± 49	10.1 ± 2.2
PRK	1491 ± 310	67.0 ± 13.9

Supplemental Table 5. Estimated Turnover Rates of CBC Intermediates in *C. reinhardtii* CC-1690 Cells.

Half-times ($T_{0.5}$) of metabolites and time to change pool sizes from low to higher light intensity were calculated based on carboxylation rates derived from measured net photosynthesis rates (338 and 771 µmol*s^{-1}*L cell $volume^{-1}$ respectively) and considering pathway stoichiometry and number of C atoms of the metabolites (Arrivault et al., 2009).

[a]CBC intermediates: the number of turnovers per molecule of RuBP synthesized.

[b]End-product synthesis: number of turnovers per molecule of CO_2 fixed, taking into account the number of carbon molecules in the metabolite and the stoichiometry of the synthesis pathway.

[c]The measured concentration of metabolite [µM] multiplied by the number of C atoms gives the concentration of C atoms in the corresponding metabolite pool.

[d]Calculation of E4P assuming equilibrium of the TRK-catalysed reaction (F6P + GAP ↔ E4P + Xu5P). For details see Supplemental Dataset 2.

[e]Duration of CO_2 fixation at the new light intensity that is required to produce the measured change in the size of that metabolite pool in the first 5 min after the increase in light intensity. The sum for all CBC metabolites is 32 s.

		Metabolite levels [µM C atoms][c]		$T_{0.5}$ [s]		Calculated duration to change pool size [s][e]
Metabolite	**Stoichiometry**	**low light**	**5min higher light**	**low light**	**5min higher light**	
RuBP	1[a]	1648.58	5485.39	2.44	3.56	11.11
3PGA	2[a]	7030.66	7715.67	20.80	10.01	3.97
GAP	2[a]	27.72	60.38	0.08	0.08	0.19
DHAP	2[a]	1021.13	2003.29	3.02	2.60	5.69
FBP	0.33[a]	636.34	470.63	0.31	0.10	0.16
F6P	0.33[a]	2320.71	4712.93	1.14	1.02	2.31
E4P	0.33[a]	53.07[d]	137.85[d]	0.03	0.03	0.08
SBP	0.33[a]	1289.95	1641.70	0.64	0.35	0.34
S7P	0.33[a]	3166.06	10157.40	1.56	2.20	6.75
R5P	0.33[a]	118.66	198.95	0.06	0.04	0.08
Xu5P+Ru5P	1[a]	113.54	193.38	0.17	0.13	0.23
G1P	0.01[b]	501.38	549.95	0.07	0.12	2.76
G6P	0.01[b]	7515.67	10029.70	1.11	0.65	-2.05
ADPG	0.034[b]	169.97	431.23	0.01	0.03	0.37
UDPG	0.034[b]	571.50	687.22	0.59	0.31	0.23

Supplemental Table 6. Carbon Sequestration into Metabolites after Transfer to Higher Light.

For details of calculation see text and Methods.

	% C sequestered into starch and metabolite in the time intervals							
	0-5min	**5-10min**	**10-20min**	**20-40min**	**40-60min**	**60-120min**	**120-240min**	**240-480min**
2OG	-0.03	0.07	0.04	-0.04	0.01	0.00	0.00	0.00
Aconitate	0.00	0.01	0.00	0.00	0.00	0.00	0.00	0.00
ADPG	0.54	0.29	-0.11	-0.03	0.01	-0.02	-0.01	0.00
Aspartate	-0.26	0.09	-0.22	-0.38	-0.02	-0.04	0.09	-0.02
Citrate	0.01	1.07	0.10	-0.10	-0.37	0.12	-0.02	-0.03
DHAP	0.76	0.05	0.05	-0.01	0.00	0.00	0.00	0.00
F6P	1.85	0.15	0.36	-0.14	-0.03	0.03	0.02	0.02
FBP	-0.13	-0.02	0.03	0.01	0.00	0.00	0.00	0.00
G1P	0.04	0.05	0.00	-0.02	0.00	0.01	0.00	0.01
G3P	0.14	0.04	0.01	-0.01	-0.02	0.00	0.00	0.00
G6P	1.94	0.63	-0.01	-0.44	-0.09	0.04	0.02	0.11
GAP	0.03	0.01	0.00	0.00	0.00	0.00	0.00	0.00
Glutamate	-0.80	2.61	1.11	-0.23	0.26	0.17	-0.01	0.06
Glycerate	0.01	-0.04	0.01	0.00	-0.01	0.00	0.00	0.00
Isocitrate	0.03	0.03	-0.02	0.02	0.00	0.01	0.00	0.00
Malate	4.52	1.27	0.54	-0.46	0.19	-0.01	0.22	0.00
PGA	0.53	2.82	-0.55	0.11	-0.09	0.11	-0.19	-0.01
R5P	0.06	0.01	0.00	-0.01	0.00	0.00	0.00	0.00
RuBP	2.96	1.82	0.10	0.31	-0.15	0.05	-0.08	-0.07
S7P	5.40	1.38	0.48	-0.31	-0.07	0.10	0.01	0.00
SBP	0.27	0.08	0.10	0.00	-0.07	0.01	0.00	-0.01
Shikimate	0.28	-0.21	0.14	-0.29	-0.01	-0.03	0.02	-0.02
Succinate	-0.27	-0.19	0.22	0.09	-0.07	-0.03	0.03	-0.02
UDPG	0.22	-0.03	0.00	-0.05	0.02	0.00	0.00	0.00
Xu5P + Ru5P	0.06	0.01	0.01	-0.01	0.00	0.00	0.00	0.00
Starch	59.70	55.79	38.89	24.97	10.11	-4.93	10.63	3.08

Supplemental References

Albe K. R. (1991). Partial Purification and Kinetic Characterization of Transaldolase from *Dictyostelium discoideum*. Exp. Myc. **1.5**: 255-262.

Badger, M.R., and Lorimer, G.H. (1981). Interaction of sugar phosphates with the catalytic site of ribulose-1,5-bisphosphate carboxylase. Biochemistry **20:** 2219-2225.

Cadet, F., and Meunier, J.C. (1988). pH and kinetic studies of chloroplast sedoheptulose-1,7-bisphosphatase from spinach (*Spinacia oleracea*). Biochem. J. **253:** 249-254.

Charles, S.A., and Halliwell, B. (1981). Light activation of fructose bisphosphatase in photosynthetically competent pea chloroplasts. Biochem. J. **200:** 357-363.

Chen, Y.R., Larimer, F.W., Serpersu, E.H., and Hartman, F.C. (1999). Identification of a catalytic aspartyl residue of D-ribulose 5-phosphate 3-epimerase by site-directed mutagenesis. J. Biol. Chem. **274:** 2132-2136.

Graciet, E., Lebreton, S., Camadro, J.M., and Gontero, B. (2003). Characterization of native and recombinant A4 glyceraldehyde 3-phosphate dehydrogenase. Kinetic evidence for conformation changes upon association with the small protein CP12. FEBS **270:** 129-136.

Iwaki T., Wadano A., Yokota A. Himeno M. (1991). Aldolase - an important enzyme in controlling the ribulose 1,5-bisphosphate regeneration rate in photosynthesis. Plant Cell Physiol. **32**: 1083-1091.

Jung, C.H., Hartman, F.C., Lu, T.Y.S., and Larimer, F.W. (2000). D-ribose-5-phosphate isomerase from spinach: Heterologous overexpression, purification, characterization, and site-directed mutagenesis of the recombinant enzyme. Arch. Biochem. Biophys. **373,** 409-417.

Kopke-Secundo, E., Molnar, I., and Schnarrenberger, C. (1990). Isolation and characterization of the cytosolic and chloroplastic 3-phosphoglycerate kinase from spinach leaves. Plant Physiol. **93:** 40-47.

Moorhead, G.B., and Plaxton, W.C. (1990). Purification and characterization of cytosolic aldolase from carrot storage root. Biochem. J. **269:** 133-139.

Roesler, K.R., and Ogren, W.L. (1990). Primary structure of *Chlamydomonas reinhardtii* ribulose 1,5-bisphosphate carboxylase/oxygenase activase and evidence for a single polypeptide. Plant Physiol **94,** 1837-1841.

Schnarrenberger, C.; Kruger, I (1986). Distinction between cytosol and chloroplast fructose-bisphosphate aldolases from pea, wheat, and corn leaves. Plant Physiol. **80**: 301-304.

Skrukrud, C.L., Gordon, I.M., Dorwin, S., Yuan, X.H., Johansson, G., and Anderson, L.E. (1991). Purification and characterization of pea chloroplastic phosphoriboisomerase. Plant Physiol. **97:** 730-735.

Sparla, F., Zaffagnini, M., Wedel, N., Scheibe, R., Pupillo, P., and Trost, P. (2005). Regulation of photosynthetic GAPDH dissected by mutants. Plant Physiol. **138:** 2210-2219.

Spreitzer, R.J., Thow, G., and Zhu, G. (1995). Pseudoreversion substitution at large-subunit residue 54 influences the CO2/O2 specificity of chloroplast ribulose-bisphosphate carboxylase/oxygenase. Plant Physiol. **109:** 681-685.

Teige, M., Melzer, M., and Suss, K.H. (1998). Purification, properties and in situ localization of the amphibolic enzymes D-ribulose 5-phosphate 3-epimerase and transketolase from spinach chloroplasts. Eur. J. Biochem. **252:** 237-244.

Thimm, O., Blasing, O., Gibon, Y., Nagel, A., Meyer, S., Kruger, P., Selbig, J., Muller, L.A., Rhee, S.Y., and Stitt, M. (2004). MAPMAN: a user-driven tool to display genomics data sets onto diagrams of metabolic pathways and other biological processes. Plant J. **37:** 914-939.

Trost P., Scagliarini S., Valenti V., Pupilio P. (1993). Activation of spinach chloroplast glyceraldehyde 3-phosphate dehydrogenase: effect of glycerate 1,3-bisphosphate. Planta **190**:321-326.

Varga, A., Szabo, J., Flachner, B., Roy, B., Konarev, P., Svergun, D., Zavodszky, P., Perigaud, C., Barman, T., Lionne, C., and Vas, M. (2008). Interaction of human 3-phosphoglycerate kinase with L-ADP, the mirror image of D-ADP. Biochem. Biophys. Res. Commun. **366:** 994-1000.

Woodrow, I.E., Murphy, D.J., and Walker, D.A. (1983). Regulation of photosynthetic carbon metabolism. The effect of inorganic phosphate on stromal sedoheptulose-1,7-bisphosphatase. Eur. J. Biochem. **132:** 121-123.